1985

Quantum Monte Carlo Study of the Thermodynamic Properties of Argon Clusters: the Homogenous nucleation of Argon in Argon Vapor and "Magic Number" Distributions in Argon Vapor

David L. Freeman
University of Rhode Island, dfreeman@uri.edu

Jimmie D. Doll

Citation/Publisher Attribution
Freeman, D. L., & Doll, J. D. (1985). Quantum Monte Carlo Study of the Thermodynamic Properties of Argon Clusters:The Homogeneous Nucleation of Argon in Argon Vapor and 'Magic Number' Distributions in Argon Vapor. *J. Chem. Phys., 82,* 462-471. doi: 10.1063/1.448768
Available at: http://dx.doi.org/10.1063/1.448768

Quantum Monte Carlo Study of the Thermodynamic Properties of Argon Clusters: the Homogenous nucleation of Argon in Argon Vapor and "Magic Number" Distributions in Argon Vapor

Quantum Monte Carlo study of the thermodynamic properties of argon clusters: The homogeneous nucleation of argon in argon vapor and "magic number" distributions in argon vapor

David L. Freeman
Department of Chemistry, University of Rhode Island, Kingston, Rhode Island 02881

Jimmie D. Doll
University of California, Chemistry Division, Los Alamos National Laboratory, MS J 569, Los Alamos, New Mexico 87545

(Received 19 July 1984; accepted 20 September 1984)

The thermodynamic properties of clusters of argon atoms are studied by a combination of classical and quantum mechanical Monte Carlo methods. The argon atoms are represented by Lennard-Jones interactions and internal energies, free energies, and entropies are calculated as a function of temperature and cluster size. For the argon system quantum effects and anharmonicity corrections are found to be simultaneously important for a temperature range from 15 to 20 K. By examining local minima in the free energy of formation of argon clusters as a function of cluster size, magic numbers in the Boltzmann mass distribution are observed at $n = 7$, 13, and 19 under some conditions of temperature and pressure. In some cases magic numbers are predicted in the quantum and not in the classical calculation. The entropy changes associated with cluster growth are found to be insensitive to cluster size. Quantum corrections are calculated to nucleation rates and found to be very important at low temperatures.

I. INTRODUCTION

It is well known that vapors at pressures supersaturated to the formation of a condensate can have exceedingly long metastable lifetimes. These long lifetimes are frequently rationalized in terms of a free energy barrier to the nucleation of molecular clusters in the vapor phase. For systems undergoing homogeneous nucleation under steady-state conditions the nucleation rate equations have been studied and several reviews of steady-state nucleation kinetics are available.[1,2] As shown in these reviews, under several reasonable assumptions, the steady state nucleation rate J, can be expressed as

$$J = \left[\sum_{n=1}^{n_{\max}} (C_n O_n)^{-1}\right]^{-1}, \tag{1}$$

where C_n is the concentration of clusters composed of n vapor phase monomers in a Boltzmann distribution, O_n is the average rate at which clusters of size n capture a monomer to grow to size $n + 1$, and $n_{\max}$ is a maximum cluster size above which contributions to Eq. (1) are negligible. Although the assumptions which lead to Eq. (1) have been challenged[3,4] and are undoubtedly inappropriate in some cases, the expression for J given in Eq. (1) is at least qualitatively accurate. The corrections required to improve Eq. (1) are peripheral to this work and we shall assume it to be appropriate. Because the sticking probability for a monomer interacting with clusters of size n is nearly unity, O_n can be calculated accurately from kinetic theory to give the expression

$$O_n = p(2\pi m k_B T)^{-1/2}(36\pi V_c^2)^{1/3} n^{2/3}, \tag{2}$$

where V_c is the effective volume per molecule, p is the pressure of the vapor phase, T is the absolute temperature, m is the mass of a monomer, and k_B is the Boltzmann constant.

In contrast to the capture probability, the concentration of clusters of size n in a Boltzmann distribution C_n is very difficult to determine and the evaluation of C_n is one of the principal theoretical problems in the study of homogeneous nucleation kinetics. Because the set of cluster concentrations in a Boltzmann distribution are equilibrium quantities, C_n can be expressed in terms of the Gibbs free energy of formation of clusters of size n, $\Delta G(n, p, T)$, by the expression

$$C_n = C_1 \exp[-\Delta G(n, p, T)/k_B T]. \tag{3}$$

The validity of Eq. (3) depends upon a number of assumptions, and to clarify those assumptions a derivation of Eq. (3) is given in the Appendix. By application of Eq. (3) the free energy barrier previously mentioned is seen to be associated with clusters of minimum concentration which give the dominant contribution to the nucleation rate in Eq. (1).

The experimental determination of cluster size distributions in a vapor is very difficult. For small metallic clusters shock tube measurements[5-8] and mass spectrometry techniques[9] have been used. For nonmetallic clusters size distributions have been determined using cluster beam methods.[10-14] One of the more intriguing observations from cluster beam experiments on rare gas systems is the identification of certain cluster sizes which are local maxima in the overall mass distribution. Cluster sizes

 0021-9606/85/010462-10$02.10

which appear as local maxima have been termed "magic numbers" and by inference have been associated with clusters of extra stability. Some of the observed magic numbers can be associated with the numbers of spheres required to form regular polyhedra.[15] Examples are the magic numbers at 13 and 55 observed for neutral xenon by Echt, Sattler, and Recknagel,[10] and also observed for ionic argon clusters by Harris, Kidwell, and Northby.[14] Other observed magic numbers are not easily interpreted. For example, magic number cluster sizes at 14 have been observed for neutral argon and krypton clusters by Ding and Hesslich.[11] The clusters in these beam experiments are formed neither at steady state nor at equilibrium, and the relation between the observed mass distributions and thermodynamic stability is not obvious. The evaluation of relative size distributions in a Boltzmann distribution for the experimentally studied cluster systems would amplify this relation. As we indicated, the relative concentrations can be extracted from the free energies of formation of clusters as a function of cluster size. Consequently free energies for clusters as a function of size provide information concerning both steady-state nucleation rates and stability information useful for the interpretation of cluster beam experiments. The evaluation of the free energy of formation of clusters and the resulting interpretation of magic numbers and nucleation rates form central goals for the work we report here.

Because of their importance to nucleation kinetics there have been a number of attempts to calculate free energies of formation of clusters theoretically. A common approach has been the application of continuum thermodynamics to cluster systems assumed to be liquid droplets.[1] The droplet model has been critiqued extensively in the literature[2] and we make no attempt to review that analysis here. It is clear that continuum models will be most deficient for smaller clusters whose geometries are not spherical and for which the atomistic nature of the clusters is important.

To determine free energies and equilibrium cluster distributions more realistically than in the continuum droplet model there have been a number of studies which take the cluster to be composed of constituent atoms and assume the forces between the atoms to be harmonic.[16,17] The most recent calculations which use the harmonic model[17] have taken the geometries of the clusters to be those determined by the minimum in the two-body additive Lennard-Jones potential surface[15] and the oscillator frequencies have been obtained by diagonalizing the Lennard-Jones force constant matrix. In the harmonic model the translational and rotational modes of the clusters are treated classically and the vibrational modes are treated quantum mechanically. The harmonic models work best at low temperatures where anharmonicity effects are least important.

To treat cluster systems with intermolecular forces that are more realistic than harmonic interactions there have been a number of studies[3,18-27] which have used a combination of Monte Carlo and molecular dynamics methods. For the rare gas systems the intermolecular forces have been taken to be pair-wise additive Lennard-Jones potentials, and the systems have been assumed to obey classical mechanics. Using classical Monte Carlo methods the free energy of formation of argon clusters as a function of cluster size has been evaluated by Lee, Barker, and Abraham[18] and recently by Garcia and Torroja.[19] In addition to the free energy barrier, Garcia and Torroja[19] determined nucleation rates for the argon system. The classical Monte Carlo and molecular dynamics studies are most accurate at high temperatures where the quantum zero point motion contributes less significantly than at low temperatures. Neither the classical Monte Carlo method nor the normal mode method is likely to be accurate at intermediate temperatures where cluster systems can be expected to be simultaneously anharmonic and quantum mechanical. An attempt has been made to include the effect of anharmonicities in a quantum calculation by Etters, Kanney, Gillis, and Kaelberer.[28] Using the self-consistent phonon approximation they calculated the thermodynamic properties of argon clusters ranging in size from 3 to 15 atoms. It is to be noted that clusters formed in beam experiments are internally cold and quantum effects are likely to be important.

In the present work we apply quantum mechanical Monte Carlo methods to the evaluation of the free energy and other thermodynamic quantities of clusters of Lennard-Jones atoms parametrized to mimic the behavior of argon. Unlike previous work on this system the application of quantum Monte Carlo methods will give results which can be expected to be accurate over the temperature range where quantum effects and anharmonicity effects are simultaneously important. The central objectives which have been met by this study are as follows:

(1) We determine the free energy of formation of clusters of argon atoms as a function of temperature to find the temperature range where both classical Monte Carlo and normal mode calculations have nonnegligible errors;

(2) we calculate the free energy of argon aggregates as a function of cluster size at low temperatures and seek magic numbers (local minima in the free energy) in the Boltzmann distribution;

(3) we assess the importance of quantum corrections to the nucleation rate at low temperature.

Our approach to the computation of fully quantum mechanical thermodynamic functions utilizes the Feynman path integral formulation of statistical mechanics.[29] Recently a number of path integral methods have been developed and implemented[30-45] to perform quantum statistical mechanical calculations on complex interacting many-body systems. In many of the approaches to quantum statistical mechanics, the path integrals have been discretized and short interval approximations have been used.[30-42] The discretized method (DISPI method) has proved to be powerful both for formal and numerical studies, and recent applications to quantum effects in a number of systems[39-41] attest to its potential utility. The DISPI formulation of statistical mechanics is known to have serious convergence difficulties when applied to systems with potential energy functions which have strong

short range repulsions.[30] The convergence difficulties associated with DISPI studies of Lennard-Jones systems have been overcome by application of an iterative matrix multiplication scheme.[36] This iterative method appears to be limited to systems with only a few quantum degrees of freedom. Another method which has been used to improve the convergence of DISPI calculations is the introduction of normal mode transformations.[36] To our knowledge the normal mode transformation technique has not been applied to systems simultaneously strongly repulsive and having a large number of quantum degrees of freedom.

We have recently developed an alternative path integral formulation of quantum statistical mechanics.[44,45] In our approach the paths are expanded in a Fourier series, and the integral overall paths is replaced by an equivalent integration overall Fourier coefficients. As we have shown by example,[45] the Fourier path integral (FOURPI) method is well converged for Lennard-Jones systems and does not suffer from the deficiencies of the DISPI approach. Because of its success for Lennard-Jones systems we have chosen the FOURPI method to evaluate the thermodynamic properties of the argon clusters examined in this work. At this writing the number of applications of path integral methods to the statistical mechanics of many-body systems with large numbers of quantum degrees of freedom is still limited. It is hoped that the results we present here using the FOURPI method will also be of use for comparison with alternative techniques.

As we have indicated in this work we carry out a fully quantum mechanical Monte Carlo study of the thermodynamic properties of clusters of argon atoms using the FOURPI method. The contents of the remainder of this paper are as follows. In Sec. II we develop the procedure used to calculate the free energy of formation of argon clusters and other thermodynamic quantities as a function of cluster size. We utilize a state integration scheme similar to that introduced by Lee, Barker, and Abraham[18] but with a continuous constraining potential more appropriate for quantum calculations. In Sec. III we present the results of our calculations on the energy, entropy and free energy of formation of argon clusters as a function of cluster size. We also determine the nucleation rates. In Sec. IV we present our conclusions.

II. METHOD

In this section we present and develop the working expressions used in the calculation of the thermodynamic properties of argon clusters. In Sec. II A we define the interaction potential used both for the intermolecular forces and in the definition of the physical clusters reported in this work. In Sec. II B we review the calculation of the thermodynamic energy when classical Monte Carlo methods are used and when the FOURPI method is used. In Sec. II C we discuss the state integrations required for the evaluation of the partition function and the Gibbs free energy.

A. The interaction potential

The subtleties associated with defining physical clusters in a vapor are well known, and working definitions have been given by Stillinger[46] and by Lee, Barker, and Abraham.[18] In the Lee, Barker, and Abraham[18] approach the clusters are defined with respect to an infinitely reflecting constraining potential about the center of mass of the system. As shown in Ref. 18, the free energies calculated with the constraining potential are insensitive to its radius with the exception of small clusters at high temperatures. The same definition of physical clusters as used by Lee, Barker, and Abraham[18] was recently used by Garcia and Torroja.[19]

In the current work we use a definition of physical clusters related to that introduced by Lee, Barker, and Abraham.[18] Because the FOURPI approach requires twice differentiable potential energy functions [see Eq. (12)], we constrain the clusters with a continuous but strongly repulsive potential centered about the center of mass. For an n-particle cluster of atoms interacting with two-body additive Lennard-Jones potentials the potential energy function V is given by

$$V(\mathbf{r}_1, \ldots, \mathbf{r}_n) = \sum_{i<j}^{n} v(r_{ij}) + \sum_{i=1}^{n} v_1(\mathbf{r}_i), \tag{4}$$

where

$$v(r) = 4\epsilon[(\sigma/r)^{12} - (\sigma/r)^6], \tag{5}$$

and

$$v_1(\mathbf{r}) = (|\mathbf{r} - \mathbf{R}_{cm}|/R_c)^{20}. \tag{6}$$

In Eqs. (4)–(6) $\mathbf{r}_i$ is the coordinate of particle i in the cluster, ϵ and σ are the standard Lennard-Jones parameters, $\mathbf{R}_{cm}$ is the coordinate of the center of mass of the cluster, given by

$$\mathbf{R}_{cm} = \frac{1}{n}\sum_{i=1}^{n} \mathbf{r}_i. \tag{7}$$

R_c is the constraining radius and r_{ij} is the distance between particles i and j. For the calculations presented here we take ϵ = 119.40 K and σ = 3.405 Å. The constraining potential $v_1(\mathbf{r})$ acts to reflect particles reaching a coordinate $|\mathbf{r} - \mathbf{R}_{cm}|$ near R_c and is essentially zero for bound particles. We have calculated the classical free energy of 13 particle clusters using the potential function defined in Eq. (4) and using the infinitely repulsive hard wall of Lee, Barker, and Abraham[18] and found complete agreement in the computed low temperature free energies to the statistical significance of the calculations.

B. Internal energy calculations

In the present work the internal energies of argon clusters are calculated using a combination of quantum and classical Monte Carlo techniques. In the classical calculations the energies are calculated from the standard expression

$$\langle U\rangle_{CM}(n,\beta) = (3n/2\beta) + \int d^3r_1\cdots d^3r_n\rho_{CM}(\mathbf{r}_1,\ldots,\mathbf{r}_n) \times V(\mathbf{r}_1,\ldots,\mathbf{r}_n)\Big/\int d^3r_1\cdots d^3r_n\rho_{CM}(\mathbf{r}_1,\ldots,r_n), \tag{8}$$

where the classical density is given by

$$\rho_{CM}(\mathbf{r}_1,\ldots,\mathbf{r}_n) = (m/2\pi\hbar^2\beta)^{3n/2}\exp\{-\beta V(\mathbf{r}_1,\ldots,\mathbf{r}_n)\}, \tag{9}$$

and V is defined in Eq. (4). In Eqs. (8) and (9) $\mathbf{r}_i$ is the coordinate of particle i, m is the mass of an argon atom and $\beta = 1/k_BT$. Equation (8) is evaluated by standard Monte Carlo methods using importance sampling.[47]

The quantum mechanical internal energies computed in this work are calculated using the FOURPI method described in detail in Ref. 45. In the FOURPI method the internal energy is calculated from the expression

$$\langle U\rangle_{QM}(n,\beta) = \int d^3r_1\cdots d^3r_n\rho_{QM} \times (\mathbf{r}_1,\ldots,\mathbf{r}_n;\ \mathbf{r}'_1,\ldots,\mathbf{r}'_n)\hat{H}|_{\substack{\mathbf{r}_1=\mathbf{r}'_1\\ \vdots\\ \mathbf{r}_n=\mathbf{r}'_n}}\Big/ \int d^3r_1\cdots d^3r_n\rho_{QM}(\mathbf{r}_1,\ldots,\mathbf{r}_n;\ \mathbf{r}_1,\ldots,\mathbf{r}_n), \tag{10}$$

where $\hat{H}$ is the Hamiltonian operator for the system,

$$\hat{H} = -(\hbar^2/2m)\sum_{i=1}^{n}\nabla_i^2 + V(\mathbf{r}_1,\ldots,\mathbf{r}_n) \tag{11}$$

and $\rho_{QM}(\mathbf{r}_1,\ldots,\mathbf{r}_n;\mathbf{r}'_1,\ldots,\mathbf{r}'_n)$ is the quantum mechanical coordinate space density matrix. As shown in Ref. 45, in the FOURPI method Eq. (10) takes the form [correcting the notational error in Eq. (16) of Ref. 45]

$$\langle\hat{H}\rangle_{k_{\max}} = \frac{3n}{2\beta} + \int d^3r_1\cdots d^3r_n\int\prod_{k=1}^{k_{\max}} d^3a_{k1}\cdots d^3a_{kn}\exp\left\{-\sum_{i=1}^{n}a_{ki}^2/2\sigma_{ki}^2\right\}\times\exp\left\{-\frac{1}{\hbar}\int_0^{\beta\hbar}V[\mathbf{r}_1(u),\ldots,\mathbf{r}_n(u)]du\right\}$$
$$\times\left[V(\mathbf{r}_1,\ldots,\mathbf{r}_n) - \frac{\hbar^2}{2}\sum_{i=1}^{n}\frac{1}{m_i}\left(\left\{\frac{1}{\hbar}\int_0^{\beta\hbar}\left(1-\frac{u}{\beta\hbar}\right)\nabla_iV[\mathbf{r}_1(u),\ldots,\mathbf{r}_n(u)]du\right\}^2 - \frac{1}{\hbar}\int_0^{\beta\hbar}\left(1-\frac{u}{\beta\hbar}\right)^2\nabla_i^2V\right.\right.$$
$$\left.\left.\times[\mathbf{r}_1(u),\ldots,\mathbf{r}_n(u)]du\right)\right]\Big/\int d^3r_1\cdots d^3r_n\int\prod_{k=1}^{k_{\max}}d^3a_{k1}\cdots d^3a_{kn}$$
$$\times\exp\left\{-\sum_{i=1}^{n}a_{ki}^2/2\sigma_{ki}^2\right\}\exp\left\{-\frac{1}{\hbar}\int_0^{\beta\hbar}V[\mathbf{r}_1(u),\ldots,\mathbf{r}_n(u)]du\right\}, \tag{12}$$

where

$$\sigma_{ki} = [2\beta\hbar^2/m(\pi k)^2]^{1/2}. \tag{13}$$

$k_{\max}$ is the number of Fourier coefficients included in the expansion of the paths and the $\mathbf{a}_{ki}$ are the expansion coefficients. The integrations over $\mathbf{r}_1$ to $\mathbf{r}_n$ and $\mathbf{a}_{k1}$ to $\mathbf{a}_{kn}$ are evaluated by Monte Carlo importance sampling techniques[47] and the one-dimensional u integrations are evaluated by Gauss–Legendre quadrature. Both Eqs. (8) and (12) can be evaluated in center of mass coordinates. Center of mass coordinates were used in the classical calculation. For the quantum calculations center of mass coordinates resulted in sampling errors in some cases and Eq. (12) was evaluated directly.

C. Free energy calculations

In this subsection we derive the expressions used to calculate the free energy of formation of the argon clusters. As shown in the Appendix for the reaction

$$n\,\mathrm{Ar}_{(g)} \longrightarrow \mathrm{Ar}_{n(g)} \tag{14}$$

the change in the Gibbs free energy is given by

$$\Delta G(n,p,T)/k_BT = -(n-1)\ln(p/k_BT) - \ln\bar{Q}(n,T) + \ln\lambda^{-3n}(T), \tag{15}$$

where the parameters are defined in the Appendix.

In this work we use internal energies computed from the methods described in Sec. II B to calculate the partition function $Q(n,\bar{V},T)$, from the expression

$$\langle U\rangle(n,T) = k_BT^2\left(\frac{\partial\ln Q(n,\bar{V},T)}{\partial T}\right)_{\bar{V}}. \tag{16}$$

In Eq. (16) $\bar{V}$ is the volume. If we integrate Eq. (16) with respect to temperature we obtain

$$\ln\bar{Q}(n,T_2) = \ln\bar{Q}(n,T_1) + (1/k_B)\int_{T_1}^{T_2}\frac{\langle U\rangle(n,T)}{T^2}dT, \tag{17}$$

where $\bar{Q}(n,T)$ is defined in the Appendix [Eq. A5)]. This same state integration procedure was used by Garcia and Torroja.[19] To evaluate the partition function at temperature T_2 we integrate Eq. (17) from a high temperature T_1 where the system is completely classical and the interatomic forces can be ignored. If we write

$$Q(n,\bar{V},T_\infty) = \lambda^{-3n}(T_\infty)\frac{n^3}{n!}q(n,\bar{V},T_\infty), \tag{18}$$

where T_∞ is a very high temperature, we obtain for the configurational integral

$$q(n, \bar{V}, T_\infty) = \int d^3r_1 \cdots d^3r_n \exp\left\{-\beta_\infty \sum_{i=1}^{n} (|\mathbf{r}_i - \mathbf{R}_{cm}|/R_c)^{20}\right\}, \quad (19)$$

where $\beta_\infty = 1/k_B T_\infty$.

If we transform Eq. (19) to center of mass coordinates

$$\mathbf{r}'_i = \mathbf{r}_i - \mathbf{R}_{cm} \quad (20)$$

we obtain

$$q(n, \bar{V}, T_\infty) = \bar{V} \int d^3r'_1 \cdots d^3r'_{n-1} \exp\left\{-\beta_\infty \sum_{i=1}^{n} (r'_i/R_c)^{20}\right\}$$

$$= \bar{V} \int d^3r'_1 \cdots d^3r'_{n-1} \exp\left\{-\beta_\infty \left(\sum_{i=1}^{n-1} r'_i/R_c\right)^{20}\right\} \quad (21)$$

$$\times \prod_{i=1}^{n-1} \exp\{-\beta_\infty (r'_i/R_c)^{20}\}. \quad (22)$$

If we define

$$\delta(n, T) = \int d^3r'_1 \cdots d^3r'_{n-1} \exp\left\{-\beta\left(\sum_{i=1}^{n-1} r'_i/R_c\right)^{20}\right\} \times \prod_{i=1}^{n-1} \exp\{-\beta(r'_i/R_c)^{20}\} \Big/ \int d^3r'_1 \cdots d^3r'_{n-1} \times \prod_{i=1}^{n-1} \exp\{-\beta(r'_i/R_c)^{20}\}. \quad (23)$$

Equation (22) becomes

$$q(n, \bar{V}, T_\infty) = \bar{V}\delta(n, T_\infty) \int d^3r'_1 \cdots d^3r'_{n-1} \times \prod_{i=1}^{n-1} \exp\{-\beta_\infty (r'_i/R_c)^{20}\}, \quad (24)$$

$$= \bar{V}\delta(n, T_\infty)\left[\int d^3r' \exp\{-\beta(r'/R_c)^{20}\}\right]^{n-1}, \quad (25)$$

$$= \bar{V}\delta(n, T_\infty)[(\pi/5)(1/k_B T_\infty R_c)^{-3/20}\Gamma(\tfrac{3}{20})]^{n-1}, \quad (26)$$

where $\Gamma(x)$ is the Gamma function.[48] The function $\delta(n, T)$ can be evaluated by Monte Carlo numerical integration.

With Eq. (26) the high temperature partition function needed for Eq. (17) is available and the partition function at lower temperatures can be evaluated by numerical integration of calculated internal energies. The calculated partition function is then introduced into Eq. (15) to calculate the free energies of formation of n-particle clusters.

III. RESULTS

In this section we present the results of our Monte Carlo investigations of the thermodynamic properties of clusters of argon atoms represented by Lennard-Jones potentials. The primary calculations were of the internal energies of the clusters from which the Gibbs free energy and other thermodynamic properties could be obtained as described in Sec. II.

For each cluster of size n an initial configuration was chosen to match the minimum energy structure reported by Hoare and Pal.[15] For the classical internal energy approximately one hundred thousand Monte Carlo moves were made followed by approximately one-million moves where data was accumulated in the evaluation of Eq. (8). In the Monte Carlo calculations the Metropolis box size[47] was chosen so that approximately 50% of the attempted moves were accepted. The constraining radius R_c required to evaluate Eq. (6) was taken to be 3σ for 2, 3, and 4 particle clusters, 4σ for cluster sizes from 5 to 16 and 5σ for cluster sizes from 17 to 20. As shown by Lee, Barker, and Abraham[18] the calculated free energies are insensitive to the choice of R_c.

In the quantum calculations the number of included Fourier coefficients in the expansion of the paths [k_{max} in Eq. (12)] was taken to be one and 4 Gauss–Legendre points were used in the u integrations. In Ref. 45 the energy of a 13 particle cluster of argon atoms at 10 K was found to be -0.01411 ± 0.0001 a.u. when k_{max} was set to 1 and -0.01413 ± 0.0002 a.u. when k_{max} was set to two. Consequently one Fourier component can be expected to be sufficient in the current calculations. In the quantum calculations the Metropolis box size[47] was chosen so that approximately 50% of the attempted moves were accepted. Moves were made in the particles and the associated Fourier coefficients simultaneously with σ_{ki} taken as the box size for the coefficients. As in the classical calculation, approximately one-hundred-thousand Monte Carlo moves were made for each cluster at each temperature from a Hoare and Pal[15] initial configuration followed by approximately one-million Monte Carlo moves to accumulate data in the evaluation of Eq. (12).

The partition functions required to determine the Gibbs free energy were evaluated from Eq. (17). The high temperature reference temperature [T_1 in Eq. (17)] was taken to be 10 000 K, which was the reference temperature used by Garcia and Torroja.[19] We extended the temperature to 20 000 K for 13 particle clusters and found no change in the calculated Gibbs free energy to the statistical accuracy of the calculation. The temperature points and weights used in the numerical evaluation of the integral in Eq. (17) were obtained from a FORTAN translation of an ALGOL program given by Gautschi.[49] The factor of T^{-2} in the integrand was incorporated into the weight function. It was found that best convergence was obtained by dividing the integration into two regions; one from T to 160 K and the other from 160 to 10 000 K. Six quadrature points in the first region and two in the second gave convergence of the integral to within the statistical errors in the calculations. In the quantum free energy calculations only energy points below 40 K were calculated with the quantum algorithm.

To assess the temperature region over which the

TABLE I. The Gibbs free energy of formation of a 13 particle cluster of argon atoms at 1 atm pressure.

T	$\Delta G_{CM}/k_BT$	$\Delta G_{QM}/k_BT$	$\Delta G_{HPW}/k_BT$[a]
10	−408.2 ± 0.3	−383.6 ± 0.4	−383.8
15	−244.4 ± 0.6	−232.0 ± 0.6	−220.3
20	−161.6 ± 0.5	−158.2 ± 0.5	−137.6
25	−117.4 ± 0.4	−115.7 ± 0.4	−87.7
30	−88.1 ± 0.5	−86.9 ± 0.5	−54.4

[a] Reference 17.

classical and normal mode approaches to the calculation of the free energy are valid, we calculated $\Delta G(n, p, T)$ as a function of T for the 13 particle clusters. The results of this series of calculations are given in Table I. In Table I the pressure was taken to be 1 atm, the free energies are given in units of k_BT, ΔG_{CM} is the classical result, ΔG_{QM} is the quantum result, and ΔG_{HPW} is the result of the quantum normal mode calculation of Hoare, Pal, and Wegener.[17] The reported error bars are single standard deviation error bars, and the same error bars will be used throughout the remainder of this paper. The Monte Carlo results agree with the normal mode results at 10 K. At 10 K the classical calculation is in error by approximately 8%. By 15 K the quantum Monte Carlo results deviate significantly from the normal mode free energies and the classical and quantum free energies agree by 30 K. We did not extend the calculation below 10 K or above 30 K because the normal mode method can be expected to be accurate below 10 K and the classical results should be sufficient above 30 K.

In Table II we give the calculated free energies in units of k_BT for argon at 10 K and 1 atm pressure as a function of cluster size. As in Table I ΔG_{CM} is the classical result, ΔG_{QM} is the quantum result, and ΔG_{HPW} is the normal mode result.[17] There is reasonable agreement between the quantum Monte Carlo results and the normal mode results for most cluster sizes. For some cluster sizes the differences between the normal mode and quantum Monte Carlo results are outside the statistical significance of the calculation. In the normal mode method the geometry of the cluster is taken from the lowest reported energy structure in the potential surface.[15] It has been argued that this structure is representative of all the other contributing structures.[17] In the Monte Carlo calculations in principle all contributing structures are included in the evaluation of Eq. (12). In practice only a fraction of the total possible structures are actually included in a Monte Carlo calculation with a finite number of points. However, the variety of structures reached in the Monte Carlo calculation may account for the differences between ΔG_{QM} and ΔG_{HPW} observed in Table II. The differences between our results and those of Hoare, Pal, and Wegener[17] for the 17 particle structure seem somewhat large and we are unable to account for this difference. In scanning the 17 particle structure to seek an explanation for the discrepancy we discovered a 17 particle structure lower in energy than that reported by Hoare and Pal.[15] The old and new 17 particle minimum energy structures are shown in Fig. 1.

TABLE II. The Gibbs free energy of formation as a function of cluster size n at 10 K and 1 atm pressure.

n	$\Delta G_{CM}/k_BT$	$\Delta G_{QM}/k_BT$	$\Delta G_{HPW}/k_BT$[a]
2	−8.19 ± 0.02	−8.03 ± 0.03	−7.59
3	−24.98 ± 0.05	−23.39 ± 0.05	−23.19
4	−50.12 ± 0.08	−46.99 ± 0.08	−46.67
5	−77.5 ± 0.2	−72.9 ± 0.2	−72.64
6	−108.6 ± 0.2	−101.5 ± 0.2	−99.30
7	−143.4 ± 0.3	−134.9 ± 0.3	−134.93
8	−175.8 ± 0.3	−165.2 ± 0.3	−164.13
9	−214.8 ± 0.5	−200.5 ± 0.8	−201.35
10	−254.6 ± 0.4	−239.1 ± 0.4	−238.94
11	−294.5 ± 0.6	−276.6 ± 0.6	−277.76
12	−346 ± 1.00	−326 ± 1.0	−324.55
13	−408.2 ± 0.3	−383.6 ± 0.4	−383.79
14	−441.1 ± 0.4	−415.3 ± 0.4	−414.73
15	−483.1 ± 0.7	−453.1 ± 0.7	−453.99
16	−526.6 ± 0.6	−495.7 ± 0.6	−494.18
17	−569 ± 1.00	−536.4 ± 0.9	−528.59
18	−620.1 ± 0.9	−583.9 ± 0.9	−581.96
19	−682.2 ± 0.8	−642.9 ± 0.8	−641.36
20	−723.5 ± 0.7	−681.4 ± 0.6	−684.23

[a] Reference 17.

The Gibbs free energy of formation of argon clusters at pressures other than 1 atm can be obtained from Table II by the expression[17]

$$\Delta G(n, p, T) = \Delta G(n, p = 1 \text{ atm}, T) + (1 - n)k_BT \ln p. \quad (27)$$

To examine $\Delta G(n, p, T)$ at pressures where the free energy maximum occurs at approximately $n = 10$, we calculated $\Delta G(n, p, T)$ from Eq. (27) and Table II at $p = 3.34 \times 10^{-14}$, 3.34×10^{-16}, and 3.34×10^{-18} atm. The results are shown in Figs. 2–4. In examining these figures it is useful to recall that local maxima in the Boltzmann mass distribution at a given temperature and pressure will be associated with local minima in the free energy of formation. At $p = 3.34 \times 10^{-14}$ atm a local minimum in $\Delta G(n, p, T)$ is observed in the quantum calculation at $n = 7$. No local minimum is seen in the classical curve. At $p = 3.34 \times 10^{-16}$ atm a local minimum is observed at $n = 13$ in both the quantum and classical calculations. At $p = 3.34 \times 10^{-18}$ atm, classical and quantum local minima are observed at $n = 13$ and a quantum local minimum is observed at $n = 19$. The magic numbers we observe in the Boltzmann mass distribution occur for cluster size where the minimum energy structures have high symmetry. As shown by Hoare and Pal,[15] the mini-

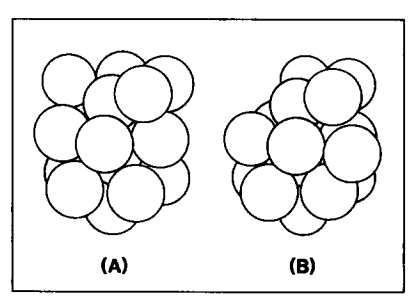

FIG. 1. The minimum energy structure for a 17 particle cluster as found by Hoare and Pal (Ref. 15) is shown in (a) [E/ϵ = 61.307] and the structure slightly lower in energy found in this work is shown in (b) [E/ϵ = 61.318].

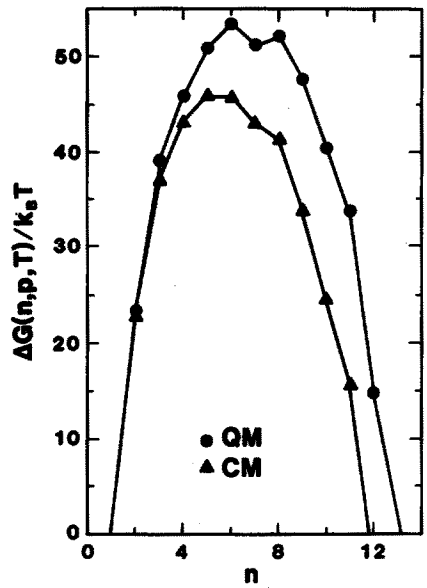

FIG. 2. The Gibbs free energy of formation as a function of cluster size at $T = 10$ K and $p = 3.34 \times 10^{-14}$ atm. The circles are the quantum results and the triangles are the classical results. The points are connected by straight lines. In no case is the error bar larger than the circle or triangle.

mum energy structure for $n = 7$ is a pentagonal bipyramid, for $n = 13$ is an icosahedron and for $n = 19$ is a "capped" icosahedron.

The sensitivity of the occurrence of magic numbers to conditions of temperature and pressure is a result of the change in the free energy of formation with temperature and pressure. At low supersaturations (pressures only slightly above the vapor pressure of pure argon) the free energy of formation rises very rapidly with cluster size and no local minima are observable for small clusters. At high supersaturated pressures the free energy of formation decreases rapidly with cluster size and no magic numbers are observable. This is seen in Table II at 1 atm pressure. Only for cluster sizes in the vicinity of the free

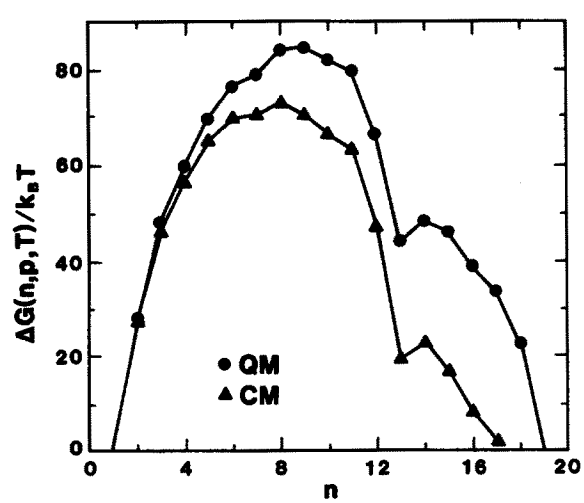

FIG. 3. The Gibbs free energy of formation as a function of cluster size at $T = 10$ K and $p = 3.34 \times 10^{-16}$ atm. The circles are the quantum results and the triangles are the classical results. The points are connected by straight lines. In no case is the error bar larger than the circle or triangle.

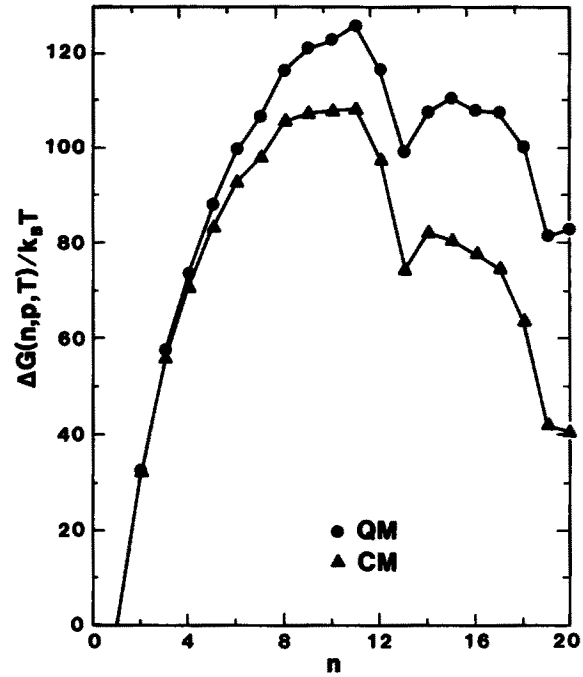

FIG. 4. The Gibbs free energy of formation as a function of cluster size at $T = 10$ K and $p = 3.34 \times 10^{-18}$ atm. The circles are the quantum results and the triangles are the classical results. The points are connected by straight lines. In no case is the error bar larger than the circle or triangle.

energy barrier are the changes in the free energy of formation small enough to observe magic numbers. At $T = 0$ K there is no barrier to nucleation and no local minima are observable in the potential energy as a function of cluster size.[15]

To gain further insight into the origin of the observed magic numbers in the Boltzmann distribution, we calculated the free energy change $\Delta\bar{G}(n, p, T)$, for the reaction

$$\mathrm{Ar}_{n-1(g)} + \mathrm{Ar}_{(g)} \rightarrow \mathrm{Ar}_{n(g)} \tag{28}$$

which is given by

$$\Delta\bar{G}(n, p, T) = \Delta G(n, p, T) - \Delta G(n-1, p, T) - \Delta G(1, p, T). \tag{29}$$

A graph of $\Delta\bar{G}(n, p, T)$ is given in Fig. 5 for $p = 3.34 \times 10^{-16}$ atm. Statistically significant local minima in the graph of $\Delta\bar{G}(n, p, T)$ are observed at $n = 7$, 13, and 19. These local minima match the observed magic numbers in the Boltzmann distribution.

To assess the origin of the observed magic numbers we have calculated the internal energy and enthalpy of argon clusters at 10 K as a function of cluster size and resolved the calculated free energies into their enthalpy and entropy components. The internal energy as a function of cluster size is given in Table III. Comparisons of the results given in Table III can be made with the self-consistent phonon approximation results of Ref. 28. In general the FOURPI results shown in Table III are higher than the self-consistent phonon results by approximately 5%. For example, the energy of the 13 particle cluster in the self-consistent phonon approximation is −463.6 in

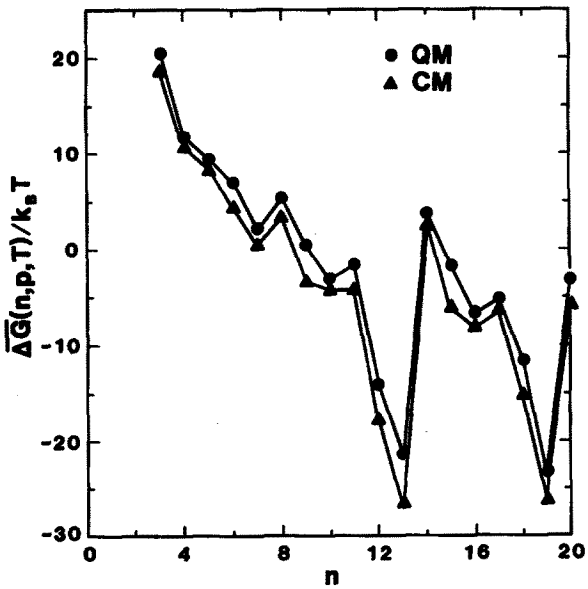

FIG. 5. The free energy change for the process $Ar_{n-1(g)} + Ar \rightarrow Ar_{n(g)}$ at $T = 10$ K and $p = 3.34 \times 10^{-16}$ atm. The circles are the quantum results and the triangles are the classical results. The points are connected by straight lines. In no case is the error bar larger than the circles or triangle.

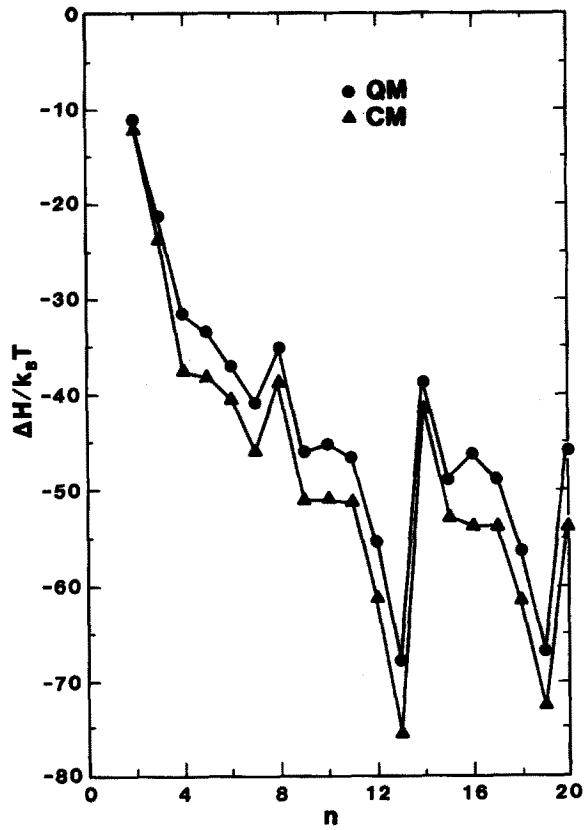

FIG. 6. The enthalpy change for the process $Ar_{n-1(g)} + Ar \rightarrow Ar_{n(g)}$ at $T = 10$ K and $p = 3.34 \times 10^{-16}$ atm. The circles are the quantum results and the triangles are the classical results. The points are connected by straight lines. In no case is the error bar larger than the circle or triangle.

units of k_BT at 10 K. The self-consistent phonon results do not include translational and rotational contributions. The additional discrepancies between the FOURPI results and the self-consistent phonon results may be caused by the lack of contributions from cubic corrections in the latter case.[50] The enthalpy change for the process given in Eq. (28) is plotted in Fig. 6 in units of k_BT. The internal energy change for the system as a function of cluster size has a similar form and is related to $\Delta H(n, T)$ by (ideal gas law assumed)

$$\Delta H(n, T) = \Delta U(n, T) - k_BT. \tag{30}$$

As with the free energy change associated with Eq. (28), the enthalpy change has local minima at the magic numbers of 7, 13, and 19. The entropy change for the process expressed in Eq. (28) is given by

$$\Delta S(n, p, T) = [\Delta H(n, T) - \Delta\tilde{G}(n, p, T)]/T \tag{31}$$

and is plotted in units of k_B in Fig. 7. Unlike the enthalpy the entropy is rather flat and shows no unusual structure at the magic numbers. It appears that the magic numbers in the Boltzmann mass distribution are associated with the favorable energies which occur for structures of high symmetry and entropic effects are relatively unimportant.

From the free energy functions plotted in Figs. 2–4, a nucleation rate can be obtained by application of Eqs.

TABLE III. The internal energy as function of cluster size at 10 K.

n	$\langle U\rangle_{CM}/k_BT$	$\langle U\rangle_{QM}/k_BT$
2	−8.32 ± 0.01	−7.23 ± 0.03
3	−29.55 ± 0.03	−26.29 ± 0.02
4	−62.14 ± 0.03	−55.52 ± 0.03
5	−95.93 ± 0.06	−85.9 ± 0.2
6	−134.2 ± 0.6	−120.7 ± 0.2
7	−178.18 ± 0.06	−159.0 ± 0.3
8	−214.2 ± 0.1	−191.7 ± 0.3
9	−262.65 ± 0.06	−235.5 ± 0.3
10	−311.05 ± 0.06	−278.5 ± 0.3
11	−359.8 ± 0.1	−323.0 ± 0.2
12	−419.1 ± 0.1	−376.2 ± 0.1
13	−491.9 ± 0.1	−441.4 ± 0.2
14	−530.82 ± 0.06	−477.5 ± 0.3
15	−581.02 ± 0.06	−523.8 ± 0.3
16	−631.7 ± 0.1	−567.7 ± 0.3
17	−682.48 ± 0.06	−613.6 ± 0.3
18	−741.7 ± 0.2	−665.8 ± 0.2
19	−811.7 ± 0.1	−730.3 ± 0.3
20	−862.7 ± 0.1	−773.9 ± 0.6

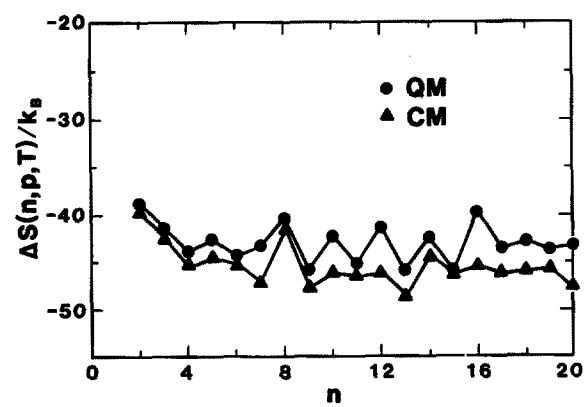

FIG. 7. The entropy change for the process $Ar_{n-1(g)} + Ar \rightarrow Ar_{n(g)}$ at $T = 10$ K and $p = 3.34 \times 10^{-16}$ atm. The circles are the quantum results and the triangles are the classical results. The points are connected by straight lines. In no case is the error bar larger than the circle or triangle.

(1)–(3). We calculated the nucleation rate at $T = 10$ K and $p = 3.34 \times 10^{-16}$ atm. From the classical free energy, we calculated a rate of $J_{CM} = (2.3 \pm 0.8) \times 10^{-26}$ m^{-3} s^{-1} and a quantum rate of $J_{QM} = (3 \pm 2) \times 10^{-31}$ m^{-3} s^{-1}. The ratio of the quantum to classical rates is

$$J_{QM}/J_{CM} = (1.3 \pm 0.8) \times 10^{-5}$$

indicating a large quantum contribution to the rates under these conditions.

IV. CONCLUSIONS

In this study we have carried out a combination of quantum and classical Monte Carlo calculations on the thermodynamic properties of clusters of Lennard-Jones atoms parametrized to mimic the behavior of argon. Our purposes in performing these calculations were to assess the importance of quantum effects on cluster systems and to search for magic numbers in the Boltzmann mass distribution. Additionally we wished to present a number of detailed results obtained with the FOURPI method that we hope will be of use for comparison with alternative techniques. Our principle conclusions are as follows:

(1) There is a temperature range over which both the quantum normal mode approximation and classical mechanics are in significant error for cluster systems. For the argon system both quantum and anharmonicity effects are important in the range of 15 to 20 K.

(2) Magic numbers do occur in the Boltzmann mass distribution for the argon system modeled by Lennard-Jones interactions. The magic numbers are observed by local minima in the free energy of formation of the clusters as a function of cluster size. The existence of magic numbers is very sensitive to conditions of temperature and pressure, and under some conditions is only observed in the quantum calculations. For the range of cluster sizes from 2 to 20 magic numbers have only been observed for high symmetry clusters ($n = 7$, 13, 19). The existence of magic numbers appears to be driven by energetic contributions, and entropic effects seem to be rather small.

(3) At low temperatures nucleation rates are sensitive to quantum effects. At 10 K and a pressure of 3.34×10^{-16} atm, the classical approximation overestimates the nucleation rate by over four orders of magnitude.

We wish to emphasize that the accuracy of our calculations is very sensitive to our ability to sample contributions from all contributing structures. The sampling problems exist for classical and quantum Monte Carlo studies and are inherent in any cluster calculation. We know of no technique to assess the extent to which all structures have been sampled efficiently. Monte Carlo calculations are likely to be more accurate than normal mode calculations which assume one contributing structure. We believe the differences between our results and those of Hoare, Pal, and Wegener[17] are at least partially explained by sampling errors inherent in the normal mode approach.

The results presented here are only one example of possible applications of the FOURPI method to quantum statistical mechanics. Other studies are currently in progress.

ACKNOWLEDGMENTS

Work at the University of Rhode Island was supported in part by grants from Research Corporation, The University of Rhode Island Academic Computer Center and The University of Rhode Island Engineering Computer Laboratory.

APPENDIX

In this appendix we derive the expression for the free energy of formation of n-particle clusters at temperature T and pressure p and the expression for the concentration of n-particle clusters in terms of the free energy of formation. The expressions given are not new[19] and are elementary. We present this derivation for completeness and to clarify the assumptions used to obtain Eq. (3). We also hope to avoid confusion with similar expressions which have led to controversy in work with the liquid droplet models of nucleation.[2]

For the reaction given in Eq. (14) the change in the molar Gibbs free energy is given by

$$\Delta G_m(n, p, T) = G_m(n, p, T) - nG_m(1, p, T), \quad \text{(A1)}$$

where $G_m(n, p, T)$ is the molar Gibbs free energy of n-particle clusters. For an ideal gas of n-particle clusters the molar Gibbs free energy is given by

$$G_m(n, p, T) = -RT \ln[Q(n, V_m, T)/L], \quad \text{(A2)}$$

where L is Avogadro's number, R is the gas constant, V_m is the molar volume, and $Q(n, \bar{V}, T)$ is the canonical partition function for ideal gas n-particle clusters. For monomers

$$Q(1, V_m, T) = V_m \lambda^{-3}(T), \quad \text{(A3)}$$

where $\lambda(T)$ is given by

$$\lambda(T) = (h^2/2\pi m k_B T)^{1/2}. \quad \text{(A4)}$$

If we write

$$Q(n, \bar{V}, T) = \bar{V}\bar{Q}(n, T) \quad \text{(A5)}$$

and use Eq. (A2), then Eq. (A1) becomes

$$\Delta G_m(n, p, T) = -RT \ln\left\{L^{n-1} \frac{Q(n, V_m, T)}{[Q(1, V_m, T)]^n}\right\} \quad \text{(A6)}$$

$$= -RT \ln\{(L/V_m)^{n-1}[\bar{Q}(n, T)/\lambda^{-3n}(T)]\} \quad \text{(A7)}$$

$$= -(n-1)RT \ln(p/k_B T) - RT \ln \bar{Q}(n, T) + RT \ln \lambda^{-3n}(T). \quad \text{(A8)}$$

In Eq. (A8) we have introduced the ideal gas law for L/V_m.

We now wish to relate the molar Gibbs free energy change in Eq. (A8) to cluster concentrations. From a grand canonical distribution it is elementary to show that[1]

$$C_n/C_1 = (C_1\bar{V})^{n-1}\{Q(n, \bar{V}, T)/[\bar{V}^n\lambda^{-3n}(T)]\} \quad \text{(A9)}$$

or

$$C_n/C_1 = (C_1\bar{V})^{n-1}\{Q(n, \bar{V}, T)/[\bar{V}^n\lambda^{-3n}(T)]\}, \quad \text{(A10)}$$

$$= C_1^{n-1}[\bar{Q}(n, T)/\lambda^{-3n}(T)], \quad \text{(A11)}$$

$$= (p/k_BT)^{n-1}[\bar{Q}(n, T)/\lambda^{-3n}(T)]. \quad \text{(A12)}$$

In obtaining Eq. (A12) we have assumed that

$$C_1 = p/k_BT, \quad \text{(A13)}$$

i.e., the vapor is an ideal gas consisting almost entirely of monomers. From Eqs. (A8) and (A12) it is clear that

$$C_n/C_1 = \exp\{-\Delta G_m(n, p, T)/RT\}. \quad \text{(A14)}$$

Equation (3) follows from Eq. (A14) by expressing the molar Gibbs free energy change as the Gibbs free energy change per cluster.

[1] F. F. Abraham, *Homogeneous Nucleation Theory* (Academic, New York, 1974).
[2] J. J. Burton, in *Modern Theoretical Chemistry*, edited by B. J. Berne (Plenum, New York, 1977), Vol. 5, p. 195.
[3] M. Rao, B. J. Berne, and M. H. Kalos, J. Chem. Phys. **68,** 1325 (1978).
[4] J. L. Katz and M. D. Donohue, Adv. Chem. Phys. **40,** 137 (1979).
[5] H. J. Freund and S. H. Bauer, J. Phys. Chem. **81,** 994 (1977).
[6] D. J. Frurip and S. H. Bauer, J. Phys. Chem. **81,** 1001 (1977).
[7] D. J. Frurip and S. H. Bauer, J. Phys. Chem. **81,** 1007 (1977).
[8] S. H. Bauer and D. J. Frurip, J. Phys. Chem. **81,** 1015 (1977).
[9] A. W. Castleman, Jr., P. M. Holland, D. M. Lindsay, and K. I. Peterson, J. Am. Chem. Soc. **100,** 6039 (1978).
[10] O. Echt, K. Sattler, and E. Recknagel, Phys. Rev. Lett. **47,** 1121 (1981).
[11] A. Ding and J. Hesslich, Chem. Phys. Lett. **94,** 54 (1983).
[12] P. W. Stephens and J. G. King, Phys. Rev. Lett. **51,** 1538 (1983).
[13] L. Friedman and R. J. Beuhler, J. Chem. Phys. **78,** 4669 (1983).
[14] I. A. Harris, R. S. Kidwell, and J. A. Northby, in *Proceedings of the 17th International Conference on Low Temperature Physics,* edited by U. Eckern, A. Schmid, W. Weber, and H. Wühl (Elsevier, Amsterdam 1984), p. 1393.
[15] M. R. Hoare and P. Pal, Adv. Phys. **20,** 161 (1971).
[16] J. J. Burton, J. Chem. Soc. Faraday Trans. 2 **69,** 540 (1973).
[17] M. R. Hoare, P. Pal, and P. P. Wegener, J. Colloid Interface Sci. **75,** 126 (1980).
[18] J. K. Lee, J. A. Barker, and F. F. Abraham, J. Chem. Phys. **58,** 3166 (1973).
[19] N. G. Garcia and J. M. S. Torroja, Phys. Rev. Lett. **47,** 186 (1981).
[20] D. J. McGinty, J. Chem. Phys. **58,** 4733 (1973).
[21] W. D. Kristensen, E. J. Jensen, and R. M. J. Cotterill, J. Chem. Phys. **60,** 4161 (1974).
[22] C. L. Briant and J. J. Burton, J. Chem. Phys. **63,** 2045 (1975).
[23] C. L. Briant and J. J. Burton, J. Chem. Phys. **63,** 3327 (1975).
[24] E. E. Polymeropoulos and J. Brickmann, Chem. Phys. Lett. **92,** 59 (1982).
[25] C. J. Briant and J. J. Burton, J. Chem. Phys. **64,** 2888 (1976).
[26] R. D. Etters and J. Kaelberer, Phys. Rev. A **11,** 1068 (1975).
[27] R. D. Etters, R. Danilowicz, and J. Kaelberer, J. Chem. Phys. **67,** 4145 (1977).
[28] R. D. Etters, L. Kanney, N. S. Gillis, and J. Kaelberer, Phys. Rev. B **15,** 4056 (1977).
[29] R. P. Feynman, *Statistical Mechanics* (Benjamin, Reading Mass., 1972).
[30] J. A. Barker, J. Chem. Phys. **70,** 2914 (1979).
[31] K. S. Schweizer, R. M. Stratt, D. Chandler, and P. G. Wolynes, J. Chem. Phys. **75,** 1347 (1981).
[32] D. Chandler and P. G. Wolynes, J. Chem. Phys. **74,** 4078 (1981).
[33] R. M. Stratt, J. Chem. Phys. **77,** 2108 (1982).
[34] M. F. Herman, E. J. Bruskin, and B. J. Berne, J. Chem. Phys. **78,** 5150 (1982).
[35] D. Thirumalai and B. J. Berne, J. Chem. Phys. **79,** 5029 (1983).
[36] D. Thirumalai, E. J. Bruskin, and B. J. Berne, J. Chem. Phys. **79,** 5063 (1983).
[37] E. C. Behrman, G. A. Jongeward, and P. G. Wolynes, J. Chem. Phys. **79,** 6277 (1983).
[38] R. A. Friesner and R. M. Levy, J. Chem. Phys. **80,** 4488 (1984).
[39] R. Kuharski and P. J. Rossky, Chem. Phys. Lett. **103,** 357 (1984).
[40] M. Parrinello and A. Rahman, J. Chem. Phys. **80,** 860 (1984).
[41] B. DeRaedt, M. Sprik, and M. L. Klein, J. Chem. Phys. **80,** 5719 (1984).
[42] R. M. Stratt, J. Chem. Phys. **80,** 5764 (1984).
[43] J. D. Doll and L. E. Myers, J. Chem. Phys. **71,** 2880 (1979).
[44] J. D. Doll and D. L. Freeman, J. Chem. Phys. **80,** 2239 (1984).
[45] D. L. Freeman and J. D. Doll, J. Chem. Phys. **80,** 5709 (1984).
[46] F. H. Stillinger, Jr., J. Chem. Phys. **38,** 1486 (1963).
[47] N. Metropolis, A. W. Rosenbluth, M. H. Rosenbluth, A. H. Teller, and E. Teller, J. Chem. Phys. **21,** 1087 (1953).
[48] M. Abromowitz and I. A. Stegun, *Handbook of Mathematical Functions,* Natl. Bur. Stand. (U.S. GPO, Washington, DC, 1964), Chap. 6.
[49] W. Gautshchi, Commun. ACM **11,** 432 (1968).
[50] R. D. Etters (private communication).